GEOCHEMICAL INVESTIGATION OF TUNGSTEN IN TWO GROUNDWATER

FLOW SYSTEMS: THE CARRIZO SAND AQUIFER, TEXAS, USA, AND THE

AQUIA AQUIFER, MARYLAND, USA

by

HEERAL B. DAVE

Presented to the Faculty of Graduate School of

The University of Texas at Arlington in Partial Fulfillment

of the requirements

for the degree of

MASTER OF SCIENCE IN ENVIRONMENTAL SCIENCE AND ENGINEERING

THE UNIVERSITY OF TEXAS AT ARLINGTON

MAY 2008

ACKNOWLEDGEMENTS

Finally, and most importantly, I would like to thank my family for their unconditional love, support, and dedication to all projects that I have undertaken so far. I will forever be grateful to my mother, Rita Dave, and my sister Ashwini Dave for all their encouragement, support and dedication over the years. Last, but not least, I would like to especially thank my husband, Philip Champion, for all his love, devotion, and interest in my project- his endless enthusiasm, logical suggestions, and eagerness to always help has made the completion of this project a reality.

April 17, 2008

ABSTRACT

GEOCHEMICAL INVESTIGATION OF TUNGSTEN IN TWO GROUNDWATER

FLOW SYSTEMS: THE CARRIZO SAND AQUIFER, TEXAS, USA, AND THE

AQUIA AQUIFER, MARYLAND, USA

Heeral B. Dave, M.S.

The University of Texas at Arlington, 2008

Supervising Professor: Karen H. Johannesson

      Groundwater sampled were collected from well sites located within the Carrizo

Sand aquifer in Atascosa and McMullen counties in Texas, and also within the Aquia

Aquifer, Maryland in the counties of Queen Anne's, Kent, and Ann Arundel in Maryland.

During the field sampling trips, on site measurements were conducted for pH, specific

conductance, temperature, alkalinity, dissolved oxygen (DO), oxidation-reduction potential (Eh), iron speciation ([Fe (II)/ Fe(III)]), and dissolved S (-II) concentrations. In order to examine and study solid phase tungsten concentrations in the Aquia (archived at the Maryland Geological Survey) and Carrizo Aquifer sediments, we collected a number of aliquots, including duplicates, from pre-existing drill cores (Evergreen Underground Water Conservation District, Pleasenton, TX; Maryland Geological Survey, Baltimore, MD). Tungsten concentrations in the Carrizo Sand Aquifer range from 3.64 to 1297 pmol kg^{-1} with the lowest concentrations reported from the recharge area followed by progressively increasing dissolved W concentrations with flow downgradient along the flow path. Total tungsten in the Aquia aquifer varies along the flow path ranging from 14.31 to 184.41 pmol kg^{-1}, with an average concentration of 80.41 pmol kg^{-1}. We suggest that increases in W concentrations in our groundwaters are reflective of pH-related desorption. Some authors, for e.g Helz and Erickson., 1999, have suggested the formation of thiomolybdates in the presence of high S(-II) values. Given that the chemistry of tungsten is very similar to that of Molybdenum, and also that the Carrizo groundwaters contain high levels of S(-II), we suggest that the possible formation of thiotungstates could most likely be responsible for the high tungsten levels in these groundwaters. Again, as was the case with our Aquia sediment samples, the high concentrations of tungsten in the last two fractions of our experiment are in accordance with these studies, and suggest that tungsten is being released into solution under oxidizing conditions.

Evolution of W in the Aquia aquifer suggests the element's conservative behavior in these generally oxic to suboxic groundwaters. The observed changes of W concentrations along the studied flow path is also consistent with some direct control due the moderately changing redox conditions in the aquifer, i.e from oxic, to suboxic conditions. We suggest therefore that for W dissolution in groundwaters, pH related adsorption/ desorption reactions are the key controlling factors in oxic, and sub-oxic waters. Our results also suggest that except for the first few sediment samples, most of the W in the Aquia sediments are bound up in Al-silicate minerals, and are therefore not available for recycling in the groundwaters.

TABLE OF CONTENTS

LIST OF FIGURES

LIST OF TABLES

CHAPTER 1

INTRODUCTION

Tungsten (W), atomic weight 74, occurs naturally as a trace element in the environment. In surface waters, tungsten occurs dominantly as the hexavalent oxy-anion tungstate (WO_4^{2-}) which is also the chief form of tungsten, found in the oxo-rich minerals scheelite ($CaWO_4$) and wolframite ($[Fe/Mn]WO_4$), (Keitzin and Adams., 1996). The hydrogeochemistry of tungsten in groundwaters, as well as the processes responsible for its mobility are poorly understood. Only a handful of authors have investigated W in the environment (Seiler at al., 2005) let alone groundwaters. The few that have conducted research on groundwaters include Grimes at al., (1995); Benson and Spenser., (1983); Johannesson at al., (2000); Seiler at.al. (2005); and Annorsen and Oskarsson. (2007). It would therefore seem that a more systematic study of W, with an emphasis on its behavior along groundwater flow paths, is necessary in order to understand the biogeochemical processes responsible for controlling W concentrations in groundwaters. It is generally agreed that the geochemistry of tungsten is similar to that of Molybdenum. BothW and Mo are Group Via transitional metals, occur in the +4, +5, and +6 oxidation states, and exhibit identical radii for their +4, +5, and +6 oxidation states (Keitzin and Adams., 1996). Naturally occurring stable isotopes of tungsten include ^{180}W ^{182}W, ^{183}W, ^{184}W, and ^{186}W.

Tungsten metal is a valuable resource because it has the highest melting point of all metals, has great strength and conductivity, and has the lowest vapor pressure of all metals making it ideal for certain industrial uses such as production of tungsten-based alloys, chemical accessories, and vacuum metallizing (http://www.goolge.com/tungsten accessed July 26th, 2008). Anthropogenic processes such as hard-metallurgy also contribute to the distribution of tungsten in the environment (Sheppard et al., 2007).

The study of tungsten in the environment has of late received considerable attention owing to its recent identification as a possible contributor to a childhood leukemia cluster in north-west Nevada (Seiler At al. 2005, Sheppard et al. 2006, 2007a, 2007b). Trace metal contents were measured in airborne particulates, groundwaters, river waters, and upwelling geothermal waters in five west central Nevada towns including Fallon, where 16 cases of childhood leukemia were diagnosed from 1997 to 2002. Tungsten was the most prominent metal in the Fallon area where W concentrations exceeded 50 µg/L thereby prompting an investigation of W in aquifers used as drinking water sources. About 68% of the study participants in the Fallon area had urine levels of W greater than the 95th percentile for a United States reference population (Seiler et al., 2005; http://www.cdc.gov/nceh/clusters/Fallon/study.htm accessed August 4th, 2003).

 The occurrence of such high concentrations of tungsten in urine samples was of immediate interest to the residents of Fallon and the CDC given that there are numerous W mines and prospects in Western Nevada, as well as the existence of an active W mill in the Fallon area that produces tungsten carbide tools (Seiler et al., 2005). It was also determined in previous studies that the source of tungsten in the airborne particles was

not natural, but instead traced to a hard-metal facility located in Fallon (Sheppard et al., 2007). However, the study is considered controversial because other authors (for e.g: Johannesson et al., 1997; Seiler et al., 2005) state that natural waters also have high W concentrations, which clearly are not anthropogenic. This would mean that the source for tungsten in the environment is a result of natural processes, rather than anthropogenic.

Because the biogeochemistry of W in the environment, and in particular, groundwater flow systems is poorly understood, a chief goal of this research is to carefully quantify W concentrations in two relatively well characterized aquifers (i.e., Carrizo Sand, Texas and Aquia aquifer, Maryland) along with redox sensitive tracers such as Fe species, S(-II), oxidation-reduction potential, dissolved oxygen, pH, and other major solute compositions in order to develop an improved conceptual model of W in the environment.

CHAPTER 2

BACKGROUND

Tungsten is a valuable commodity because it has the highest melting point of all metals, great strength and conductivity (Kletzin and Adams, 1996). Tungsten based alloys, with a hardness comparable to that of diamond, are major industrial products, and the metal is also used widely in producing electric lights, and as a lubricating agent (Kletzin and Adams, 1996) . The annual percentage of tungsten used per year in the US is 35,000 metric tons. However, this value fluctuates depending on the need of the space and military industries (Kletzin and Adams, 1996).

It was only very recently that tungsten's role in biological systems was recognized (Keltzin and Adams, 1996). The first indications were reported in the early 1970s when the growths of certain *clostridia* were stimulated by the addition of tungsten in their growth media (Ljungdahl, 1976; Kletzin and Adams, 1996). Since then, more than 10 tungstoenzymes have been experimentally isolated, and there is reason to expect that this number will increase in the near future with additional study. In contrast to W, the essential role of the chemically comparable element molybdenum (Mo) in a variety of fundamental biological processes (Mo-containing enzymes used for nitrogen fixation) has been known in the last 60 years (Bergmeyer et al., 1993). Prior to the discovery of functional W-containing proteins, it was suggested that replacing the Mo in molybdoenzymes with W might provide insight into the role of the metal tungsten in particular catalytic processes. However, studies carried out on the influence of W on

4

microorganisms investigated, resulted in no catalytic activity, and it was determined that although Mo and W were high in their degree of chemical similarity, organisms were highly selective such that even if W does become incorporated into a molybdoenzyme, its properties are different enough from Mo, with only a few exceptions, to preclude significant catalytic activity (Kletzin and Adams, 1996).

Tungsten is a refractory siderophile element whose initial abundance in the Earth can be estimated from chondritic abundances (Newsom et al., 1996) without a volatile correction. Tungsten behaves as a highly incompatible lithophile element, in magmas, and thus is severely depleted in the upper mantle and enriched in the continental crust (Newsom et al., 1996). Because tungsten is not in the subduction component, it is extracted into the continental crust due to its incompatibility during partial melting (Newsom et al., 1996). Tungsten is usually found in the natural environment as oxo-rich tungstate minerals scheelite ($CaWO_4$) and Wolframite ($[Fe/Mn]WO_4$) (Kletzin and Adams, 1996). More reduced forms of tungsten, such as tungstite ($[WS_2, W(IV)]$) are rare in nature (Kletzin and Adams, 1996). Tungsten deposits are usually a result of hydrothermal mineralization and metamorphic processes, typically found in sub-terranean environments as opposed to marine environments, and W can be deposited at the discharge site of thermal waters (Ivanova, 1986; Gilbert et al., 1992; Kletzin and Adams, 1996).

In surface waters, the effective solubility of W is much lower than that of Mo due to stronger sorption and/or co-precipitation of W onto minerals, such that W concentrations rarely exceed 20 nM, whereas Mo concentrations could be two or more

orders of magnitude higher (Krauskoph, 1970; Ivanova, 1986; Johannesson et al, 2000). Tungsten is present in significant amounts in 4 types of waters: (1) groundwaters associated with W-containing ore deposits; (2) alkaline, nitrogenous fissure-vein thermal waters of crystalline rocks; (3) alkaline waters of lakes in arid zones; and (4) hot-spring waters and hydrothermal vents (Kletzin and Adams, 1996).

Recently it has been found that deep-sea or hydrothermal vents represent unique environments where there is an increase in W concentrations and availability resulting from convective circulation of seawater through newly formed volcanic crust at seafloor spreading centers. In contrast, Mo is removed from seawater during hydrothermal recycling (Kennish and Lutz, 1992; Trefry et al, 1994; Kletzin and Adams, 1996). It was found that W, in contrast to Mo, was present in samples of vent fluids at about one thousand times that found in seawater (Kletzin and Adams, 1996).

CHAPTER 3

LOCATION, GEOLOGY AND HYDROGEOLOGY

<u>2.1 The Aquia Aquifer</u>

The Aquia aquifer is a coastal plain aquifer outcropping along a northwest trend from approximately Washington, DC towards Baltimore and Annapolis, MD (Fig. 1). The Aquia dips to the southeast beneath the Chesapeake Bay (Apello, 1995). The Aquia Formation is Paleocene in age. For the purpose of this study, well samples, and investigations of groundwater sampling for Tungsten analysis was carried out on Maryland's eastern shore (Fig. 1).

The Aquia aquifer thickens towards the southeast and consists predominantly of clay, silt and sand (Hansen 1974). In terms of abundance, the mineralogy of the aquifer is primarily composed of quartz sand, followed by 10- 40% glauconite, some shell fragments, as well as minor amounts of lignite, clay minerals, garnet, magnetite, hornblende, and pyrite. The resulting green color produced from glauconite has led numerous investigators to refer to it as the "Aquia greensand" (Chapelle 1983).

The aquifer is confined between two clay layers: the Marlborough clay overlying the aquifer, and the underlying Severn Formation. The Aquia formation is approximately 31 - 46 m thick, acts as a water table aquifer in the regions where it outcrops, but is largely confined to the east at its surface exposure. The Chesapeake Bay and Potomac River, which are much lower elevation, and therefore serve as discharge areas reflecting potentiometric lows (Chapelle 1983). Groundwater recharged in the outcrop area, in

northern Kent County, on Maryland's eastern shore, flows south and southeast towards the Chesapeake Bay as indicated by the pre-developed potentiometric surfaces (Drummond, 2001; Curtin, et al., 2002).

Purdy et al, 1996 suggest that based on ^{14}C and [36]Cl/Cl measurements, the upper part of the Aquia aquifer groundwaters are about 18,000 a in age, whereas the lower part of the Aquia aquifer groundwaters are as old as 100,000 a (Purdy et al., 1996). The flow pattern of the aquifer indicates that it is made up of 3 distinct water compositions. Previous geochemical investigations of Aquia groundwaters delineate three distinct zones of groundwater composition (Chapelle, 1983). Zone 1 is parallel to the outcrop area and is about 42 km wide and is characterized by relatively high calcium (~30 mg/L), magnesium (~10 mg/L), and bicarbonate (~150 mg/L) concentrations. This region is further characterized by its low sodium concentrations (~2 mg/L). Region 2, which occurs downgradient along the flowpath is about 38 km wide and characterized by relatively constant bicarbonate levels, increasing sodium, decreasing calcium, and decreasing magnesium concentrations. Region 3, which is located down gradient from region 2, and consists of low calcium (~2 mg/L), low magnesium (~1 mg/L), high bicarbonate (~300 mg/L), and high sodium (~100 mg/L) concentrations (Chapelle 1983).

Aquia Aquifer: Wells Sampled
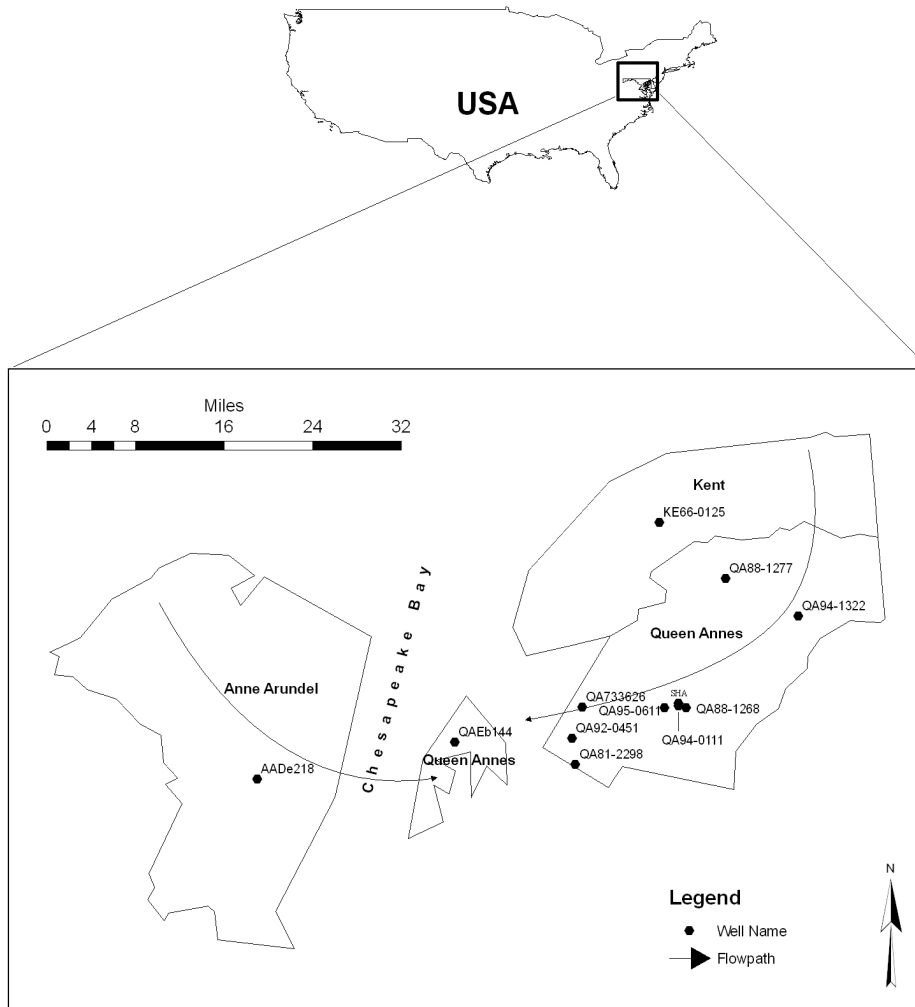
Figure 1: Map of the USA showing location of Maryland. Inset presents study area within central and east central Maryland showing investigated flow path, and locations of wells sampled.

2.2 The Carrizo Aquifer

The Carrizo aquifer is a confined sand aquifer, and predominantly consists of unconsolidated fine- to- medium grained Eocene quartz sand. It also contains small amounts of clay, lignite, calcite, and pyrite. The estimated porosity of the Carrizo ranges between 30 to 40% (Pearson and White, 1967). The aquifer crops out in a band nearly paralleling the Gulf Coast along Southern Texas. The aquifer contains freshwater at depths greater than 1500 m dipping southeast (Tang and Johannesson, 2006).

Well samples, and investigations of groundwater sampling for Tungsten analysis was carried out within Atascosa and McMullen counties located in southern Texas (Fig. 2). Wells tapping the aquifer were chosen within these counties with regard to their availability, and accessibility. The main source of recharge into the aquifer is rainfall, and this takes place at the recharge zone located in Northern Atascosa County, from where the water flows down-dip in the south easterly direction (Tang and Johannesson, 2007). According to Hamlin (1988) the hydraulic conductivity of the Carrizo Sand aquifer ranges from ~20.4 m/day near the recharge zone to ~2.4 m/day in the down-dip region.

The groundwater chemistry of the Carrizo aquifer is affected by a number of processes that include: 1) dissolution of calcium carbonate; 2) dissolution of chloride salts; 3) oxidation of organic matter; 4) dissolved ferric and sulfate ion reduction in the deeper waters of the aquifer, and 5) chemical weathering of Al-silicate minerals along the down-gradient direction of the flowpath (Hamlin, 1988).

Carrizo Aquifer: Wells Sampled
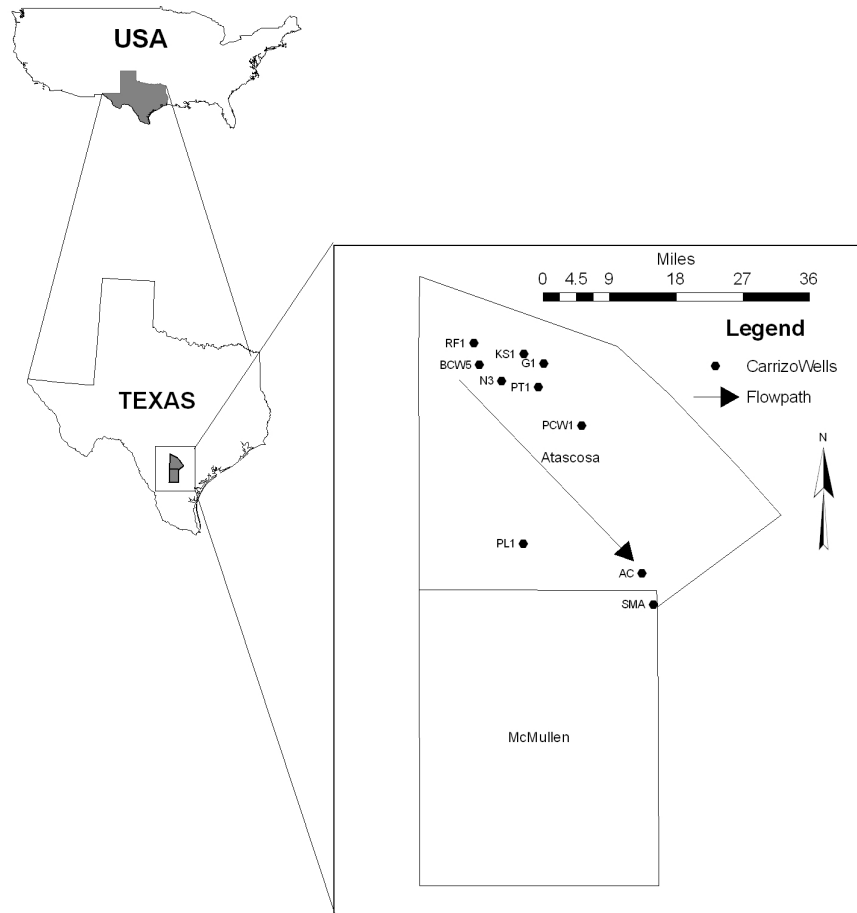
Figure 2: Map of the USA showing location of Texas. Inset show location of study area within Texas. Subset presents outcrop area, investigated flow path of groundwater, and location of wells sampled in the Carrizo Sand Aquifer.

CHAPTER 4

MATERIALS AND METHODS

<u>4.1 Sample Locations</u>

Groundwater sampled were collected from well sites located within the Carrizo

Sand aquifer in Atascosa and McMullen counties in Texas, and also within the Aquia

Aquifer, Maryland in the counties of Queen Anne's, Kent, and Ann Arundel in Maryland.

Carrizo water samples were collected in March, 2006 along the same general flow path

previously studied by other researchers (Pearson and White, 1967; Castro et al., 2000;

Castro and Goblet, 2003; Vessely, 2004; Tang and Johannesson, 2006; Haque and

Johannnesson, 2006). Aquia water samples were also collected along a specific flowpath

in June 2006, previously studied by other authors (Haque at al., 2008). From each well

site, the groundwater samples were collected and analyzed for W concentrations. Along

with the samples, a field blank consisting of MilliQ water, as well as three duplicate

samples of various wells were also collected.

<u>4.2 Preparation of Sampling Materials</u>

Prior to transportation and collection, all field HDPE sample bottles, LDPE

cubitainers and Teflon® tubing were acid washed in the laboratory using trace element

clean procedures (Johannesson et al, 2004). During the field sampling trips, on site

measurements were conducted for pH, specific conductance, temperature, alkalinity,

dissolved oxygen (DO), oxidation-reduction potential (Eh), iron speciation ([Fe (II)/

Fe(III)]), and dissolved S (-II) concentrations. Prior to sample collection, all wells were purged at high capacity for 30 minutes to remove water from the well bore. In order to ensure that samples represented groundwaters from the Carrizo Sand and Aquia aquifers, and not from their well bores. Water temperature, specific conductance, and pH were also closely monitored during the purging process, and sample collection did not commence until these parameters were stable. Iron speciation [Fe(II) and Fe(III)], S(-II), dissolved silica, Mn, dissolved oxygen, N species (NH_4^+ and NO_3^-) were quantified using separate sample aliquots via UV/VIS spectrophotometry using a portable spectrophotometer (Tang and Johannesson, 2006; Haque and Johannesson, 2006; Basu et al., 2007; Haque et al., 2008).

Each of these parameter was calibrated and the sample concentration verified using a series of calibration standards of known concentrations. Fe (II) was determined using the 1,10 Phenanthroline method (Eaton et al., 1995a), total iron [Fe_T] was determined by the Ferrozine method (Stookey, 1970; Hach, 2004), and Fe (III) was subsequently determined by the difference [$Fe(III) = Fe_T - Fe(II)$]. The method detection limits for Fe_T and Fe(II) are 0.16 µmol kg^{-1} and 0.36 µmol kg^{-1}, respectively (Hach, 2004). Dissolved sulfide, S(-II) concentrations were determined using the Methylene Blue method (Eaton et al.,1995a). The detection limit for $S(-II)^-$ is 0.16 µmol kg^{-1} (Eaton et al., 1995a). Dissolved oxygen concentrations were was determined using the High Range dissolved oxygen method (method detection limit: 18.8 µmol kg^{-1}; Hach 2004) and Carmine methods (method detection limit: 0.38 µmol kg^{-1}; Hach, 2004). The detection limit for DO is 18.8 µmol kg^{-1}. Concentrations of dissolved Si, Mn, NO_3^-, and

13

NH_4^+ were determined using the PAN method, Heteropoly Blue Method, and Cadmium

Reaction Method respectively (Hach, 2004). The method detection limits for Si, Mn,

NO_3^- and NH_4^+ are 0.36 µmol kg^{-1}, 0.13 µmol kg^{-1}, 0.16 µmol kg^{-1}, and 0.55 µmol kg^{-1}

respectively (Hach, 2004).

4.3 Tungsten Collection

Handling of bottles in the field were carried out by wearing two sets of

polyethylene gloves, and collection of groundwater samples was similar at all well sites.

Previously cleaned (trace metal) cubitainers were rinsed three times with groundwater

from the well pump-head, before filling the cubitainer with groundwater from the well.

The collected samples were then filtered through 0.45 µm filters (German Science,

polyether sulfone membranes). Cleaned 1L LDPE bottles were rinsed three times with

filtered groundwater from the cubitainer prior to collection of the filtered sample water

for laboratory analysis. Groundwater samples for tungsten analysis were then acidified to

pH < 2 using ultrapure nitric acid (Seastar Baseline) to prevent precipitates from forming

and thereby preserving the samples. Filtered and acidified samples were than stored at

~4°C until analysis.

4.4 Sediment Sampling

In order to examine and study solid phase tungsten concentrations in the Aquia

(archived at the Maryland Geological Survey) and Carrizo Aquifer sediments, we

collected a number of aliquots, including duplicates, from pre-existing drill cores (Evergreen Underground Water Conservation District, Pleasenton, TX; Maryland Geological Survey, Baltimore, MD). For the Aquia aquifer, we subsampled aliquots from sampling depths of 61m, 72m, 78m, 86.5m, 97m, and 105m (see Haque at al., 2008 for details). The Carrizo sand aquifer samples were collected from the following ranges: 900-930m, 930-960m, 960-990m, and 990-1030m, respectively, from a recently drilled well. Collected sediment samples were also stored at ~4°C in precleaned ziplock-style plastic bags until analysis. To minimize contamination, all samples were collected by wearing two sets of gloves, and using plastic tools and clean polyethylene bags (e.g., Haque at al., 2008).

4.5 Tungsten Analyses

4.5.1 Groundwater tungsten analysis:

All collected groundwater samples for W concentrations were analyzed at Old Dominion University (Norfolk, VA, Dr. Z. Chen, analyst) using high resolution inductively coupled mass spectrometry (HR-ICP-MS, Finnigan MAT ELEMENT 2). Two W isotopes (^{182}W and ^{183}W) were monitored during the analysis because they have no direct isobaric interferences and interference corrections for polyatomic ions are minimal. The instrument was calibrated and the sample concentrations were verified using a series of W calibration standards ranging from 0 to 1000 µg/l, and analytical precision was typically better than 3.24% RSD (relatively standard deviation). W calibration standards were prepared from high purity single element stock solutions

(High-Purity Standards, Charleston, SC, USA). In order to avoid instrument drift, all standards and sample solutions were spiked with 4.0 ppb indium acting as an internal standard.

4.5.2 Sequential extraction analysis:

In order to characterize the distribution of tungsten in the Aquia and Carrizo sediments, all samples were evaluated using a modified sequential extraction procedure described by Tang et al. (2004). The procedure was used to examine W in five "operationally defined phases" within the sediment including exchangeable, acidic, reducible, oxidizable and residual phases of W within the collected sediment samples. Briefly (from: Tang et al., 2004):

Fraction 1: Exchangeable phase- refers to trace elements weakly associated with clays, hydrated oxides of iron and manganese, and humic acids, and are readily mobilized by changes in ionic strength. Briefly, a 0.59 aliquot of sample was extracted into a 50 ml tube with 8 ml of 1 M CH_3COONa at room temperature. The mixture, which was also at pH 8.2, was then agitated on shaker for 1 hr.

Fraction 2: Acidic phase- refers to elements that are bound to sediment carbonates, which are susceptible to carbonate dissolution as sediments are acidified. Briefly, the residue from the previous fraction (fraction 1) was then leached at room temperature with 8 ml of CH_3COONa adjusted to a pH of 5.0 with CH_3COOH. The mixture was subsequently agitated on a shaker for 5 hrs.

Fraction 3: Reducible phase- refers to trace elements that are bound to iron and manganese hydroxides, which will be reduced and solubilized under anoxic conditions. Briefly, the residue from fraction 2 was extracted with 20 ml of 0.04 M $NH_2OH.HCL$ in 25% (v/v) CH_3COOH for 6 hrs at $96\pm1^{o}C$. The mixture was subsequently agitated on a shaker for 30 minutes.

Fraction 4: Oxidizable phase- refers to trace elements that are in reduced metal complexes, or bound to organic matter, which can be subsequently released into solution under oxidizing conditions. Briefly, the residue from fraction 3 was extracted with 3 ml of 0.02 M HNO_3 and 5 ml of 30% H2O2, adjusted to a pH of 2.0 with ultrapure HNO_3 (Seastar Chemicals). The mixture was heated to $85\pm1^{o}C$ for 2 hours with occasional agitation. The mixture was then cooled to room temperature after which 5 ml of 3.2 M CH_3COONH_4 in 20% (v/v) HNO_3 was added, and the mixture was then diluted to 20 ml and agitated on a shaker for 30 minutes at room temperature.

Separation was effected by centrifugation at 10,000 rpm for 10 minutes between each successive fraction. The supernant was then removed and stored in a 50 ml bottle at 4oC until analysis was carried out. The residue from each section was then washed with 8 ml of distilled de-ionized (18 MΩ cm) MilliQ water (Q-water). After centrifugation of 20 minutes, this second supernant was discarded.

Fraction 5-R: Residual phase refers to trace elements that are held within the crystal structure of primary and secondary minerals, which are not expected to be released into the solution over a reasonable time span under natural conditions. Briefly, the residue from fraction 4 was digested in a 50 ml Teflon® beaker with 10 ml of

ultrapure HF (Seastar Chemicals). The mixture was then evaporated to near dryness. Subsequently, 10 ml of ultrapure HNO3 (Seastar Chemicals) was added and again, the mixture was evaporated to near dryness. The residue was then dissolved with Q-Water and diluted up to 25 ml with Q-water. Thereafter, another 10 ml of ultrapure HF was added and the mixture was evaporated to near dryness. The residue was then dissolved with Q-water and diluted up to 25 ml with Q-water.

Finally, 0.2 g of initial sediment sample of dry weight was digested according to the same procedure for the residual phase, and the final solution was diluted to 25 ml with Q-water.

CHAPTER 5

RESULTS

5.1 The Carrizo Sand Aquifer

Groundwater samples from the Carrizo sand aquifer are depicted in Tables 1, 2 and Figures 3 and 4. Concentrations of W, redox sensitive species such as Fe(II), Fe(III), S(-II), Mn, oxidation-reduction potential, and general geochemical parameters (pH and TDS) for Carrizo sand groundwaters are presented in Tables 1 and 2, and plotted as a function of distance along the flow path in Figs 3 and 4. pH values of groundwater samples range from 6.1 to 8.6. The first 15km of the flow path exhibit variations in pH between 6.1 and 6.4. At a distance of >40km, further downgradient groundwater pH progressively increases reaching values > 8.5 (Fig.3). Alkalinity (presented as HCO_3) changes along the flow path of the Carrizo Aquifer ranges from 0.63 mmol kg^{-1} to 5.76 mmol kg^{-1}. More specifically, along the first 15km of the flow path, alkalinity varies from 0.63 mmol kg^{-1} to 1.3 mmol kg^{-1}, and subsequently increases to values up to 5.76 mmol kg^{-1} from distances of greater than 26 km up to 65.8 km (Fig 1).

Within the Carrizo sand aquifer Fe_T varies from below detection to a high of 54.4 µmol kg^{-1} [i.e., Peeler well] (Table 2). It is important to point out that during the 2006 sampling campaign, observations in the Peeler well suggested that either the pump was not working properly, or the well integrity had somehow been compromised (e.g., Basu at al., 2007). Specifically, unlike the clear groundwater samples collected from the Peeler well during previous sampling campaigns (e.g., Tang and Johanesson, 2005, 2006; Haque

19

and Johanesson., 2006a), groundwater abstracted from the well in March 2006 contained abundant orange to brown colored, fine-grained (i.e. silty) sediment, which did not clear even after purging the well for more than an hour. The color of the suspended sediments was suggestive of Fe(III)- rich minerals. Filtration of the sample through a 0.45 µm pore size filter (see sec 3.1 above), however, removed the sediment from the groundwater, permitting collection of a clear groundwater sample. Nonetheless, because the iron concentration measured on site was substantially greater than previous measurements (e.g., Fe_T for 2003 and 2004 was 8 µmol kg^{-1} and 14.3 µmol kg^{-1} respectively, vs. 54.4 µmol kg^{-1} for 2006; Tang and Johanesson, 2005, 2006), I will use an average of the more consistent, previous Fe measurements for Peeler well groundwaters (See Basu et al. 2007). Closer to the recharge zone, between 0 and 15 km, total iron varies widely from 0.73 µmol kg^{-1} to 31.6 µmol kg^{-1}. At 0.5 km along the flow path (well F-1) , the concentration of Fe_T is 13.8 µmol kg^{-1} and at 4.3 km (well BCW-5) along the studied flow path, the concentration increases slightly to 15.8 µmol kg^{-1}. Further down gradient along the flow path, the concentration drops to 0.73 µmol kg^{-1} at 7.4 km (well KS-1). At a distance of 9.4 km (well N-3) Fe_T rises again to 11.5 µmol kg^{-1} and then to 31.6 µmol kg^{-1} at a distance of approximately 13.0 km (well G-1). Beyond well G-1, FeT forst decreases sharply to 24.0 µmol kg^{-1} at a distance of approximately 15 km (Poteet well), and then decreases more gradually along the remainder of the flow path to values < 1 µmol kg^{-1} by the end of the 66 km flow path (Fig. 4, Table 2). Ferrous iron, Fe (II), is the dominant form of iron (Fe) observed along the flow path in the Carrizo Sand aquifer, and ranges from below detection limit (i.e.,< 0.36 µmol kg^{-1}) to 11.2 µmol Kg^{-1} (Table 2, Fig

4). Ferric iron concentrations [calculated from the differences between Fe_T and Fe (II)] range from 0.01 µmol kg^{-1} to 9.3 µmol kg^{-1}. Regions closer to the recharge zone, approximately the first 15 km of the flow path, generally exhibit higher concentrations of Fe (II) relative to Fe(III). The only exception, is well BCW-5 (4.2 km), where the Fe (III) concentration (8.2 µmol Kg^{-1}) is greater than the Fe (II) concentration of 7.5 µmol kg^{-1}. Ferrous iron concentrations increase downgradient at wells PCW-1 (26.1 km) and Peeler-1 (41.1 km) except for wells AC74R-2 at a distance of 59.0 km and SMA74R-1 at a distance of 65.8 km, where the Fe (III) is higher than the Fe (II) concentrations.

Dissolved S(-II) concentrations in the Carrizo Sand Aquifer groundwaters range from below detection (0.16 µmol kg^{-1}) to approximately 20.0 µmol kg^{-1} (Table 1, Fig 2). Between 0.5 km and 9.3 km along the flow path (wells F-1 and N-3), concentrations are below detection. Downgradient, beyond well N-3, the S(-II) concentration increases to 0.75 µmol kg^{-1} at a distance of 12.8 km (well G-1). The increase in dissolved sulfide is followed by a subsequent decrease in concentrations to 0.56 µmol kg^{-1} at 14.5 km (Poteet well). With flow beyond 14.5 km, the S(-II) concentration begins to increases reaching concentrations of up to 19.9 µmol kg^{-1} at approximately 66 km (well SMA74R-1). Between 59 km and 65.8 km (wells AC74R-1 and SMA74R-1), the S(-II) concentrations show a sharp increase from 5.6 µmol kg^{-1} to 19.9 µmol kg^{-1}.

Manganese (Mn) concentrations along the studied flow path within the Carrizo Sand aquifer range from 0.2 µmol kg^{-1} to 3.8 µmol kg^{-1}. Proximal to the recharge zone (approximately the first 15 km of the flow path), Mn concentrations are low and range from 0.2 µmol kg^{-1} and 1.7 µmol kg^{-1}. Further along the flow path, beyond 15 km,

concentrations increase reaching the highest value of 3.83 µmol kg^{-1} at well PCW-1 (26.1 km). Beyond 26 km, the Mn concentrations decrease along the flow path, and show variations at the last 3 wells [Peeler (41.1 km), AC74R-2 (59 km) and SMA74R-1 (65.8 km)] ranging from 0.45 µmol kg^{-1} to 2.9 µmol kg^{-1}.

Oxidation- reduction potential (Eh) values for the Carrizo aquifer groundwaters range from -110 mV to 327 mV (Table 2, Fig. 2). In close proximity to the recharge zone the Eh values are higher than the Eh values measured in groundwaters further downgradient (Fig. 4). Further along the flow path, Eh values drop to 48 mV at a distance of 26 km (well PCW-1). Still further downgradient, the oxidation-reduction potential drastically decreases reaching negative values.

5.1.1 Tungsten concentrations (groundwater samples):

Table 1 and Fig. 2 present W concentrations, as well as their distribution, in the Carrizo Sand aquifer as a function of distance from the recharge area. Tungsten concentrations range from 3.64 to 1297 pmol kg^{-1} with the lowest concentrations reported from the recharge area followed by progressively increasing dissolved W concentrations with flow downgradient along the flow path (Fig. 4).

Table 1: Groundwater properties of the studied wells in the Carrizo Sand aquifer

Samples	Distance (Km)	Conductivity µS cm^{-1}	Temperature ºC	TDS	pH	Eh mV	Alkalinity µmol kg^{-1}
F-1	0.5	559	24.7	358	6.46	264	1.3
BCW-5	4.29	302	24.61	193.6	6.16	233	0.63
KS-1	7.4	334.6	23.79	214	6.3	327	1.03
N-3	9.37	166.2	26.2	107.8	6.21	190	0.65
G-1	12.8	273.5	25.8	175.2	6.31	133	0.86
Poteet	14.5	386.7	28.24	247.3	6.36	155	0.86
PCW-1	26.1	589.5	34.26	377.5	7.2	48	4.07
Peeler-1	41.1	495	27.3	316.5	8.7	-110	3.38
AC74R-2	59	974	55	623	8.61	-135	5.28
SMA	65.8	1050	31.82	672.2	8.54	-110	5.76

Table 2: Concentration and speciation data for dissolved Fe, S (-II), and Mn in the groundwaters from the Carrizo Sand aquifer

Samples	W pmol kg^{-1}	Fe$_T$ µmol kg^{-1}	Fe(II) µmol kg^{-1}	Fe(III) µmol kg^{-1}	S^{2-} µmol kg^{-1}	Mn µmol kg^{-1}
F-1	78.7	13.84	12.36	1.49	0.09	0.8
BCW-5	9.46	15.75	7.52	8.23	0.09	1.02
KS-1	3.64	0.73	0.72	0.02	BDL	0.2
N-3	16.3	11.57	11.28	0.29	0.09	0.75
G-1	18.1	31.653	30.62	1.03	0.75	0.59
Poteet	1.90	24.16	17.19	6.97	0.56	1.7
PCW-1	27.4	19.51	10.21	9.3	1.15	3.83
Peeler-1	246	54.44	11.2	BDL	2.56	2.9
AC74R-2	780	0.24	BDL	0.24	5.61	0.45
SMA	1297	0.96	0.36	0.6	19.93	1

BDL= Below Detection Limit

Table 3: Concentrations of major solutes, U and Re for the Carrizo Sand Aquifer- adapted from Tang and Johannesson (2006)

	KS-1	N-3	Poteet	PCW-1	Peeler-1	AC74R-2	SMA
Well depth (m)	122	182.9	289.6	487.7	655.3	1316.7	1420.4
Latitude	29° 5' 57.7"N	29° 2' 48.1"N	29° 2' 4.2"N	28° 57" 34.8"N	28° 43' 44.2"N	28° 40' 14.2"N	28° 38' 41.6"N
Longitude	98° 36' 9.6"W	98° 34' 44.4"W	98° 34' 25.9"W	98° 29' 19.8"W	98° 36' 11.3"W	98° 22' 17.2"W	98° 20' 42.4"W
T (°C)	25.7	28.4	27.8	32.9	28.1	35.9	47.8
DOC (umol/kg)	14.2	25.8	68.3	21.7	15.8	54.2	23.3
Ca (mmol/kg)	0.63	0.38	0.76	2.01	0.45	0.06	0.08
Mg	0.2	0.12	0.23	0.33	0.36	0.01	0.01
Na	1.12	0.71	1.16	1.15	3.96	8.74	10.24
K	0.13	0.13	0.2	0.14	0.15	0.05	0.06
Si	0.38	0.29	0.27	0.23	0.26	0.43	0.48
Cl	1.43	1.06	1.44	0.87	0.37	1.23	1.78
SO4	0.27	0.22	0.36	0.37	0.35	0.79	0.71
PO$_4$ (umol/kg)	<0.04	<0.4	1.85	<0.4	1.77	<0.4	<0.4
[CO$_3^{2-}$]$_F$[b]	0.23	0.03	0.15	6.17	57.6	202	105
U (nmol/kg)	0.31	0.01	0	0.01	0	0	0.01
Re	0.04	0.03	0.01	0.01	0.03	0.01	0.02

BDL= Below Detection Limit
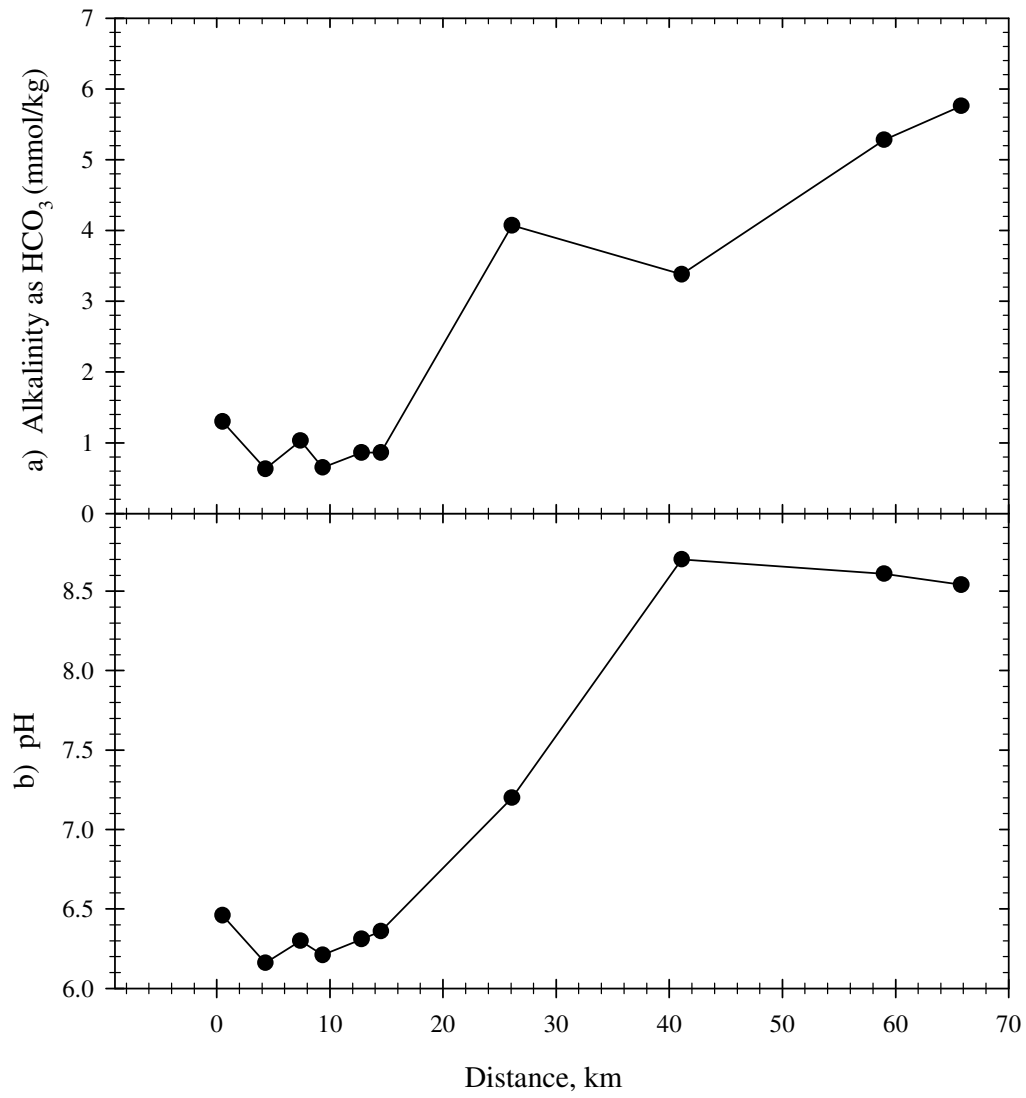
Figure 3: Carrizo aquifer data: a) alkalinity; b) pH as a function of distance (km) from the recharge zone.
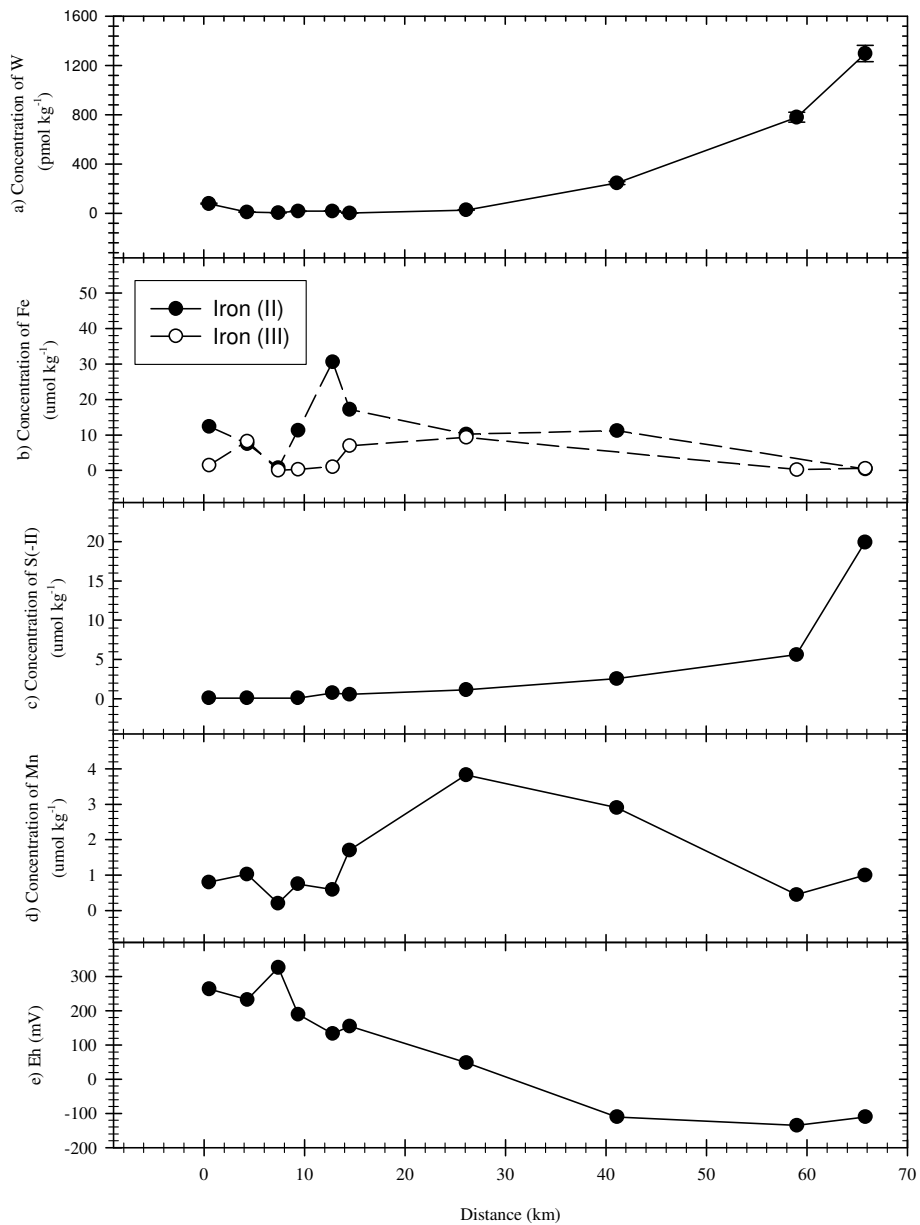
Figure 4: Carrizo aquifer data: a) W concentrations; b) Fe speciation; c) S(-II) concentrations; d) Mn concentrations; and e) Eh as a function of distance (km) from the recharge zone.

5.1.2 Sequential extraction analysis of the Carrizo sediments:

The results for the sequential extraction analysis for W in the Carrizo Sand aquifer

sediments are summarized in Table XX. Below we present the results of the sequential

extraction procedure in the order of each successive fraction:

Fraction 1: In the Carrizo sediment samples, concentrations of total exchangeable

adsorbed W range from 3 to 44 pg g^{-1} (Table 3). Overall, the exchangeable portion of W

represents the second lowest concentrations of total extractable W (Fig. 3).

Fraction 2: Concentrations of total W bound to carbonates ranges from 0

(essentially below detection) to 1 pg g^{-1} (Table 3). This fraction accounts for the lowest

concentration of total extractable W (Fig. 3).

Fraction 3: Concentrations of total extractable W associated with iron and

manganese oxides ranges from 14 to 59 pg g^{-1} (Table 3). This fraction accounts for the 3rd

highest fraction of total extractable W (Fig. 3).

Fraction 4: Concentrations of total extractable W bound to organic matter, or in

sulfide minerals, ranges from 230 to 796 pg g^{-1} (Table 3) and accounts for the 2nd largest

fraction of total extractable W (Fig. 3).

Fraction 5: Concentration of total extractable W in the residual phase ranges from

580 to 3042 pg g^{-1} (Table 4) accounting for the largest fraction of total extractable W.

Table 4: Concentrations of extractable W in sediment samples collected from the Carrizo Sand aquifer at depths of 900-930m, 930-960m, 960-990m, and 990-1030m respectively.

	Units	C 900-930	C 930-960	C 960-990	C 990-1030
F1	pg g^{-1}	3.000	18.000	9.000	44.000
F2	pg g^{-1}	0.000	1.000	0.000	0.000
F3	pg g^{-1}	36.000	59.000	14.000	57.000
F4	pg g^{-1}	796.000	502.000	560.000	230.000
F5- Residual	pg g^{-1}	580.000	951.000	776.000	3042.000
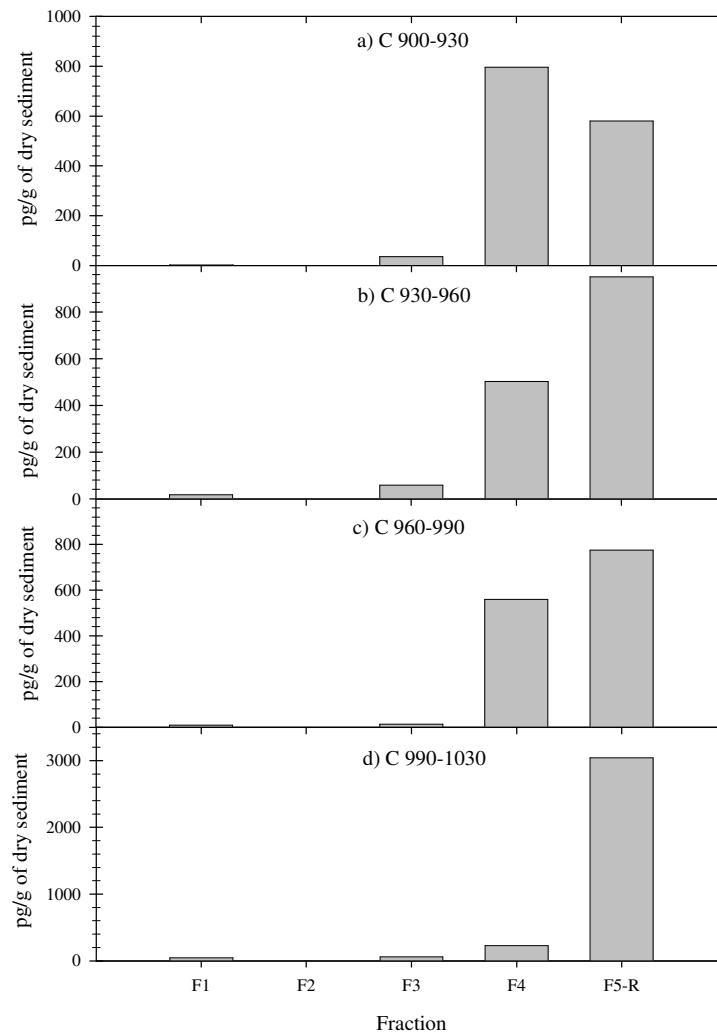
Figure 5: Fractionation of W in the Carrizo Sand sediments at wells a) C900-930; b) C 930-960; c) C 960-990; and d) C 990-1030 respectively:

28

5.2 The Aquia Aquifer

Geochemical parameters, including dissolved W concentrations measured in groundwaters collected from the Aquia aquifer are represented in Tables 4 and 5, and plotted as a function of distance along the flow path in Figs. 6 and 7. The pH of Aquia groundwaters range from neutral to slightly alkaline. Alkalinity, is expressed as HCO_3, and ranges between 2.0 and 4.0 mmol kg^{-1}. Both pH and alkalinity exhibit overall increases with flow along the flow path (Fig. 6)

Dissolved oxygen concentrations remain relatively low throughout the Aquia aquifer ranging from 9.4 to 51 µmol kg^{-1} except for one well located on the eastern shore (well AA DE 218) with a concentration of 124 µmol kg^{-1} (Table 4, Fig. 7). Eh values range from -53 to 61 mV with Eh values typically being higher near the recharge zone compared to groundwaters collected from downgradient along the flow path in the aquifer (Table 4, Fig. 7). Nitrate (NO_3^-) concentrations range from below detection, to 15 µmol kg^{-1} (Table 5, Fig. 8), whereas NH_4^+ concentrations range from 0.37 to 15.1 µmol kg^{-1}.

Total dissolved iron concentrations, Fe_T, range from below detection to 18 µmol kg^{-1}. Fe (II) concentrations range from below detection to 9.9 µmol kg^{-1}, whereas the Fe (III) concentrations range from below detection to 14.5 µmol kg^{-1}. Fe (III) predominates in groundwaters collected along the first 52 km of the flow path, presumably as colloids (e.g. Hofmann abd Liang, 2007), whereas beyond 52 km, Fe (II) becomes the dominant form of Fe (Table 5, Fig. 7). There is a noticeable sharp transition at 52 km where this change from Fe (III) to Fe (II) occurs (Haque et al., 2008).

Dissolved sulfide [S (-II)] ranges from below detection to 0.52 μmol kg^{-1} remaining generally low along the flow path (Table 5, Fig. 7). This feature sets the Aquia aquifer apart from the Carrizo Sand aquifer which exhibits relatively high S(-II) concentrations near the end of the studied flow path (Fig. 4).Therefore, the Aquia aquifer groundwaters are sub-oxic and never become sulfidic, whereas the Carrizo Sand groundwaters do become sulfidic. Mn concentrations in the Aquia aquifer range from below detection to 0.44 μmol kg^{-1}, also remaining generally low along the entire flow path (Table 5, Fig. 7). NH$_4$ concentrations range between 0.42 to 15.1 μmol kg^{-1} remaining generally high throughout the aquifer along the flow path (Table 5, Fig. 7).

5.2.1 Tungsten concentrations (groundwater samples)

Total tungsten varies along the flow path ranging from 14.31 to 184.41 pmol kg^{-1}, with an average concentration of 80.41 pmol kg^{-1} (Table 5 and Fig. 7). At this point we would like to stress that the W concentrations are much lower than those found in the groundwaters of the Carrizo Sand aquifer, and they also do not show a systematic variation along the flowpath and tend to fluctuate irregularly.

Table 5: Groundwater properties of the studied wells in the Aquia aquifer

Sample	Distance- Km	Temperature °C	pH	Eh mV	DO mmol kg⁻¹	Alkalinity mmol kg⁻¹
KE660125	22.5	7.57	7.57	25.5	51 ± 1.80	1.99
QA881277	33.5	7.73	7.69	44	13.5 ±0.21	2.79
QA941322	36.2	8.1	8.01	-11	19.6 ±0.10	3.08
AADe218	40	14.49	7.81	60.5	124 ± 1.80	3.24
QA881268	51.2	8.08	8.08	-10.5	16.7 ±0.07	2.48
SHA	52	8.38	8.38	-46	21.4 ± 0.12	3.19
QA940111	52.5	16.17	7.91	-3	11.1 ±0.05	2.91
QA950611	55	16.09	8.02	-18	50 ± 0	3.79
QA733626	64.5	7.84	7.84	27.5	23.2 ±0.12	2.98
QA812298	70.7	8.3	8.3	-11	20.3 ± 0.05	3.60
QA920451	75.1	7.93	7.93	11.5	12 ± 0.10	3.90
QAEB144	86.3	16.24	8.12	-53	9.39 ± 0.08	4.16

Table 6: Concentration and speciation of dissolved Fe, S (-II), Si, Mn, NH_4^+ and NO_3^- in the groundwaters of the Aquia aquifer

Sample	W pmol kg⁻¹	Fe_T µmol kg⁻¹	Fe(II) µmol kg⁻¹	Fe(III) µmol kg⁻¹	S^{2-} µmol kg⁻¹	Si mmol kg⁻¹	Mn µmol kg⁻¹	NH_4^+ µmol kg⁻¹	NO_3^- µmol kg⁻¹
KE660125	30.7	12.7 ± 0.21	0.9 ± 0.03	11.8 ± 2.58	BDL	1.26±0.05	1.01± 0	0.42±0.19	BDL
QA881277	184	17.7 ± 0.01	7.7 ± 0	10 ± 0.27	0.23 ± 0.02	0.41 ± 0.00	0.14± 0.01	2.03±0.19	0.48 ± 0
QA941322	90.9	15.4 ± 0.05	2.8 ± 0.1	12.5 ± 0.34	BDL	0.32 ± 0.00	BDL	14.8±0.00	1.13 ± 0
AADe218	93.3	14 ± 0.01	5.31 ± 0.1	8.7 ±0.23	0.52 ± 0.02	0.37± 0.00	0.76± 0.02	0.37±0.00	0.32 ± 0
QA881268	6.50	14.7 ± 0.08	0.18 ± 0	14.5 ± 0.40	0.1 ± 0.02	0.44±0.00	0.42±0	9.12±0.93	0.32 ± 0
SHA	22.4	7.01 ± 0.06	2.49 ± 0.1	4.36 ± 0.12	0.4 ± 0.02	0.24± 0.00	BDL	6.77±0.00	3.23 ± 0
QA940111	14.3	11.4 ± 0.1	6.8 ± 0.1	4.6 ± 0.12	BDL	0.23± 0.00	BDL	3.22±0.00	BDL
QA950611	41.5	3.35 ± 0.02	3.35 ± 0.09	BDL	BDL	0.57± 0.00	BDL	4.83±0.00	0.75±0.09
QA733626	132	BDL	BDL	BDL	BDL	0.44± 0.00	0.43± 0.01	7.73±0.00	1.13 ± 0
QA812298	10.9	9.94 ± 0.03	9.94 ± 0.27	BDL	0.34 ± 0.03	0.2±0.00	0.04± 0	15.1±0.00	0.65 ± 0
QA920451	16.6	9.01 ± 0.01	9.01 ± 0.24	BDL	BDL	0.38± 0.00	BDL	9.02±0.00	0.48 ±0
QAEB144	124	8.28 ± 0.01	4.71 ± 0.13	3.58 ± 0	0.16 ± 0	0.22±0.00	0.11± 0.01	1.39±0.19	0.32 ± 0

BDL= Below Detection Limit

Table 7: Concentrations of major solutes for the Aquia aquifer

| Solutes	F	Cl	PO$_4$	SO$_4$	Li	Na	K	Mg	Ca
Units	mmol/kg	mmol/kg	mmol/kg	mmol/kg	mmol/kg	mmol/kg	mmol/kg	mmol/kg	mmol/kg
KE660125	0.0094	0.1052	BDL	0.1270	BDL	0.085	0.056	0.083	0.925
QA881277	0.0074	0.0621	0.00454	0.0774	BDL	0.179	0.072	0.137	1.422
QA941322	0.0264	0.0257	BDL	0.0280	BDL	0.382	0.313	0.647	0.943
AADe218	0.0055	0.0700	BDL	0.0518	BDL	0.037	0.087	0.054	1.597
QA881268	0.0229	0.0217	BDL	0.0386	BDL	0.484	0.362	0.601	0.715
SHA	0.0177	0.0426	BDL	0.0423	BDL	2.391	0.152	0.230	0.317
QA940111	0.0166	0.0530	BDL	0.0583	0.00294	0.348	0.393	0.752	0.985
QA950611	0.0187	0.0395	BDL	0.0708	BDL	0.355	0.323	0.532	0.810
QA733626	0.0102	0.0573	BDL	0.0412	0.00340	0.358	0.239	0.525	1.246
QA812298	0.0358	0.0375	BDL	0.0537	0.00297	0.607	0.363	0.548	0.669
QA920451	0.0253	0.0406	BDL	0.0502	0.00347	2.134	0.306	0.583	0.733
QAEB144	BDL	BDL	BDL	0.0772	BDL	1.833	0.060	0.313	1.232

BDL= Below Detection Level
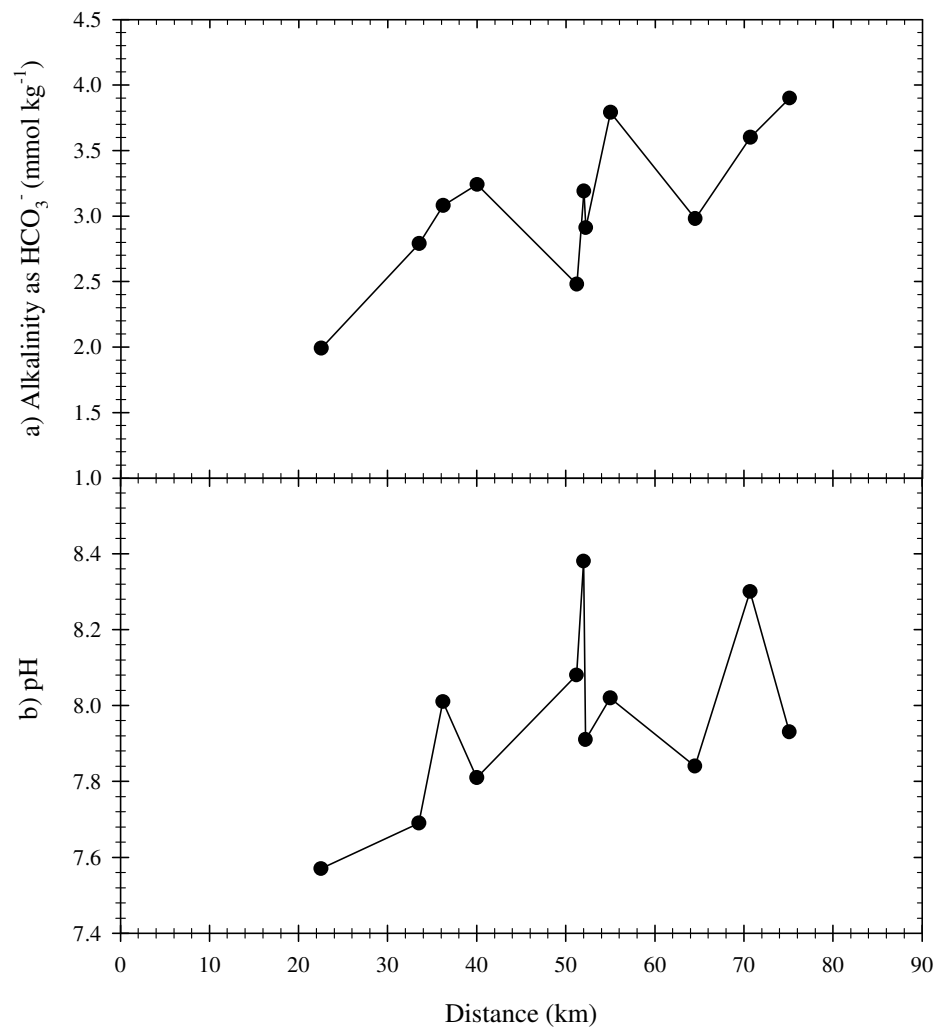
Figure 6: Aquia Aquifer data: a) Alkalinity and b) pH as a function of distance (km) from the recharge zone.
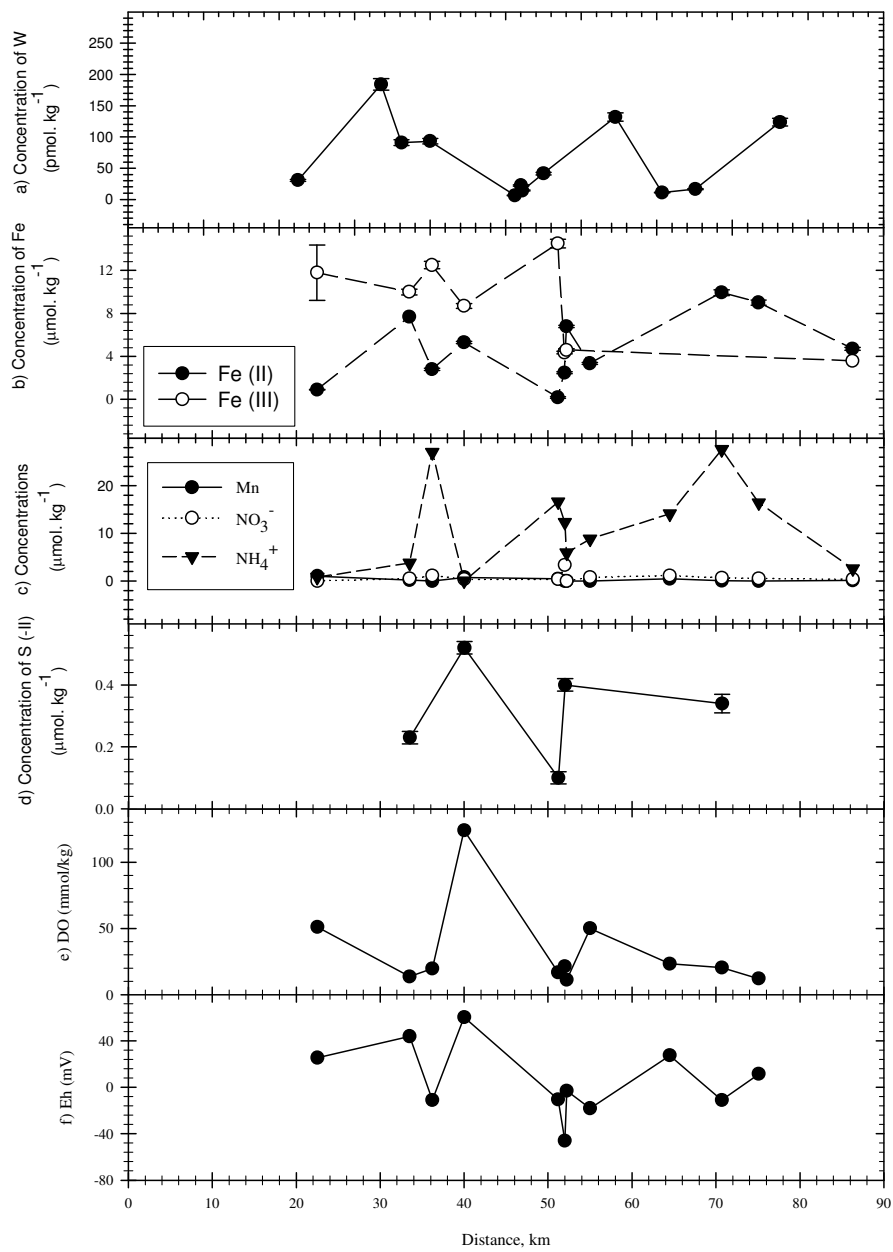
Figure 7: Aquia aquifer data: a) W concentrations; b) Fe speciation; c) Mn, NO_3^-, NH_4^+ concentrations; d) S(-II) concentrations; e) Dissolved Oxygen concentrations; and e) Eh as a function of distance (km) from the recharge zone.

5.2.2 Sequential extraction analysis of the Aquia sediments.

The results for the sequential extraction analysis for W in the Aquia aquifer sediments are summarized in Table X. Below we present the results of the sequential extraction procedure in the order of each successive fraction:

Fraction 1: In the Aquia sediment samples, concentrations of total exchangeable adsorbed W range from 16 to 49 pg g^{-1} (Table 6). Overall, the exchangeable portion of W represents the second lowest concentrations of total extractable W (Fig. 6).

Fraction 2: Concentrations of total W bound to carbonates ranges from 2 to 65 pg g^{-1} (Table 6). This fraction accounts for the third lowest concentration of total extractable W (Fig. 6).

Fraction 3: Concentrations of total extractable W associated with iron and manganese oxides ranges from 0 (essentially below detection) to 44 pg g^{-1} (Table 6). This fraction accounts for the lowest fraction of total extractable W (Fig. 6).

Fraction 4: Concentrations of total extractable W bound to organic matter ranges from 216 to 1810 pg g^{-1} (Table 6) and accounts for the 2nd largest fraction of total extractable W (Fig. 6).

Fraction 5: Concentration of total extractable W in the residual phase ranges from 287 to 2280 pg g^{-1} (Table 6) accounting for the largest fraction of total extractable W (Fig. 6).

Table 8: Concentrations of extractable W in sediment samples collected from the Aquia aquifer at depths of 61m, 78m, 86.5m, 97m, and 105m respectively.

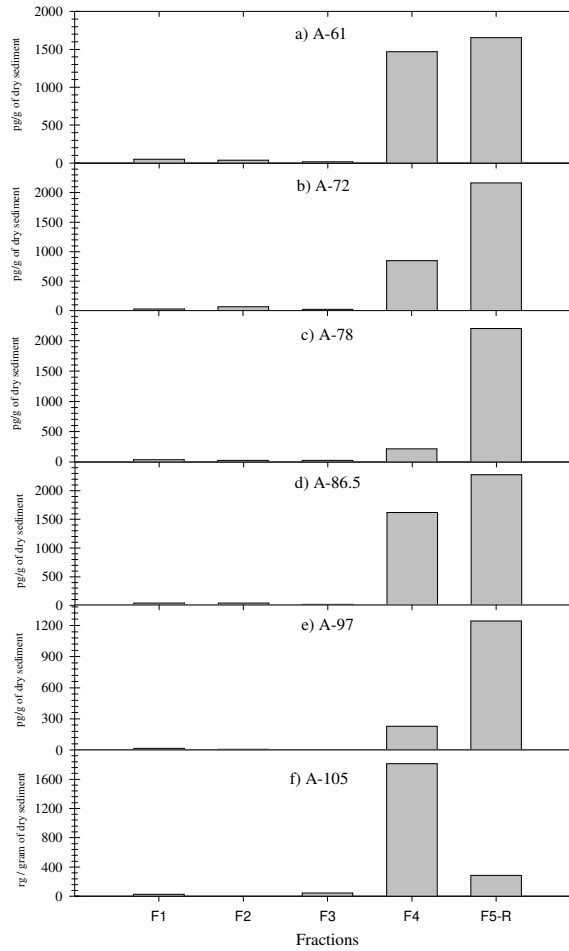| Fraction	Unit	A-61	A-72	A-78	A-86.5	A-97	A-105
F1	pg g^{-1}	49.0	26.0	35.0	39.0	16.0	28.0
F2	pg g^{-1}	38.0	65.0	25.0	40.0	8.00	2.00
F3	pg g^{-1}	18.0	24.0	28.0	16.0	0.00	44.0
F4	pg g^{-1}	1470	846	216	1620	229	1810
F5-Residual	pg g^{-1}	1650	2170	2200	2280	1240	287

Figure 8: Fractionation of W in the Aquia sediments at wells a) A-61; b) A-72; c) A-78; d) A-86.5; e) A-97; and f) A-105 respectively

CHAPTER 6

DISCUSSION

6.1 The Carrizo Aquifer

6.1.1 Controls of redox along the Carrizo flow path:

The chemical composition of the Carrizo groundwaters change systematically with flow down gradient. Within the first 10 – 15 km, measured Eh and dissolved oxygen concentrations vary greatly as do other field parameters such as iron concentration and speciation, and dissolved sulfide concentrations. Proximal to the recharge zone (i.e 10- 15 km), dissolved Fe concentrations fluctuate between 1.43 to 32.5 µmol kg^{-1} compared to portions further down the flow path that range between 1.25 and 39.6 µmol kg^{-1} (Fig. 4). The measured values suggest that Fe (III) reduction is occurring closer to the recharge zone and further down gradient because: (i) Fe concentrations are generally high, and (ii) Fe (II) is the predominant Fe species in groundwaters with high total iron concentrations (Haque et al., 2008). More specifically, between 0.5 and 4.3 km (wells F-1 and BCW-5; Fig. 4), the data is indicative of substantial Fe(III) reduction as the Fe(II) concentrations increase by a factor of almost 7. However, between 4.3 and 7.4 km (wells BCW-5 and KS-1), Fe concentrations decrease abruptly suggesting that Fe(II) oxidation has occurred at these wells with subsequent precipitation of Fe(III) oxides/oxyhydroxides. The observed decrease in concentrations of Fe(II) does not appear to reflect precipitation of Fe(II)- sulfide minerals given that S(-II) concentrations are low and have not yet changed in comparison to groundwaters collected further along the flow path. The oxidation-

37

reduction potential is observed to be highest at well KS-1 with a value of 327 mV indicating relatively oxidizing conditions (Haque and Johannesson., 2006).

With flow beyond 7.4 km (well KS-1), the data is consistent with the occurrence of redox zones dominated by Fe reduction and progressively followed by sulfate reduction within the aquifer (e.g., Back and Barnes, 1965; Champ et al., 1979; Edmunds et al., 1984; Haque and Johannesson., 2006; Lovely and Goodwin., 1988). Between 7.4 and 9.37 km (wells KS-1 and N-3), ferrous iron [Fe (II)] concentrations increase from below detection to 11 μmol kg^{-1} indicating Fe(II) reduction. At 12 km (well G-1) ferrous iron concentration increase to 30 μmol kg^{-1}, decrease at 14.5 km (Poteet well), and then exhibit a steady decline in concentrations up to 41 km at Peeler well to values close to the detection limit for the remainder of the flow path indicating redox conditions being buffered by Fe(III) reduction in this portion of the aquifer (Fig. 4).

Comparable to Fe concentrations, sulfide [S(-II)] concentrations also range from below detection [S(-II) = < 1 μmol kg^{-1}] at well KS-1, increase slightly in groundwaters at 9.4 km (well N-3), and then begin to steadily increase beyond 26 km at well PCW-1 (Fig. 4). Unlike dissolved Fe concentrations, however, S(-II) concentrations increase by a factor of 3 between 26.1 and 41.1 km (wells PCW-1 and Peeler-1) then consequently increases by a factor of 8 between 59 and 66 km (wells Peeler-1 and SMA) further down gradient likely buffering redox conditions between these two wells. Previous authors (eg. Haque and Johannesson, 2006) state that Fe and sulfide data for the Carrizo aquifer are consistent with a zone of predominantly Fe(III) reduction between 9.4 and 41 km (wells N-3 and Peeler-1), and a zone of chiefly sulfate reduction beyond 59 km (well AC74R-1).

6.1.2 Hydrogeochemical controls on W distribution in the Carrizo groundwaters:

Evolution of W in the groundwaters of the Carrizo indicate concentrations that range from 1.9 to 1297 pmol kg^{-1}, reveling a progressively increasing trend from the recharge area, and along the entire flow path (Fig. 4). The observed changes in the concentration of tungsten are consistent with changes in pH, and controls of redox on the aquifer, i.e. from suboxic to anoxic/sulfidic conditions. For example, along the first 25 km of the flow path, W concentrations remain low peaking at about 1.90 pmol kg^{-1} (Fig.4). These values are consistent with the pH values from 0 to 25 km that range between 6.46 and 7.2 (Fig. 3 and Table 1) such that low W concentrations correspond to lower pH values. Other authors (e.g Seiler at al, 2005; Lassner and Shubert, 1999) suggest that W adsorption/desorption is strongly dependant on pH, and that at low pH values, W is readily adsorbed to Fe and Mn hydroxides/oxyhydroxides, as well as Fe sulfides, thus lowering dissolved W concentrations in groundwaters. The authors also state that polymerization of WO_4^{2-} (tungstate) takes place with increasing pH thereby increasing concentrations of dissolved W in groundwaters forming polytungstate species. Seiler at al, (2005) state that as pH values increase from about 8.0, W bound to metal oxides is desorbed and subsequently released into solution. Our study indicates that as flow progresses downgradient along the flow path, tungsten values increase substantially, peaking at values as high as 1297 pmol kg^{-1}, again positively correlating to increased values in pH and S(-II). Our studies indicate that as the pH increases from about 8.0 to 8.54, the sorbed percentage of tungsten decreases dramatically, and as a result, we have increased values of dissolved W concentration in our groundwater samples. We suggest

that increases in W concentrations in our groundwaters are reflective of pH-related desorption. Some authors, for e.g Helz and Erickson., 1999, have suggested the formation of thiomolybdates in the presence of high S(-II) values. Given that the chemistry of tungsten is very similar to that of Molybdenum, and also that the Carrizo groundwaters contain high levels of S(-II), we suggest that the possible formation of thiotungstates could most likely be responsible for the high tungsten levels in these groundwaters.

6.1.3 Assessing mobilization of tungsten from sequential extraction results of the Carrizo sediments:

As with the sequential extraction of the Aquia sediments, our Carrizo sediment results demonstrate that tungsten bound to metal complexes or organic matter (oxidizable portion) and the residual portion (tungsten held within the crystal strucuture of primary and secondary minerals) represent the major portion of total extractable tungsten. On the other hand, the exchangeable/labile, acidic/ W bound to sediment carbonates, and reducible/W bound to Fe and Mn hydroxides fractions represent the minor portion of our total extractable tungsten (Fig. 5). Our sequential extractions results are in general agreement with previous studies that found that W was roughly distributed equally in the oxidizable and residual fractions (e.g Koutsospyros et al., 2005).

Again, as was the case with our Aquia sediment samples, the high concentrations of tungsten in the last two fractions of our experiment are in accordance with these studies, and suggest that tungsten is being released into solution under oxidizing conditions. We suggest that the most important source of W in these groundwaters can

either be W associated with organic matter as sulfate reducers continue to oxidize the organic matter thereby reducing SO_4^{2-} to sulfide. Alternatively, the Fe oxides in these sediments may be sufficient to oxidize metal sulfides containing W, and hence leading to the release of W to the water. The results are consistent with previous studies demonstrating that reduced metal complexes, organic material and crystal structures of minerals are hosts for non-labile forms of tungsten (Tanizaki at al, 1009; Kist., 1994).

6.2 The Aquia Aquifer

6.2.1 Redox conditions in the Aquia aquifer:

The chemical composition of the groundwaters in the Aquia aquifer changes systematically with flow down-gradient. The aquifer ground waters are characterized by increasing alkalinity and pH due to chemical weathering of silicates, including glauconite, and dissolution of shell materials along the flow path (Chapelle, 1983). Chapelle and Knobel report that the Aquia groundwaters are of the Ca-Mg-HCO$_3$ type (for the first 42 km of the studied flowpath) and evolve towards Na-HCO$_3$ type waters at around 80 km (Chapelle and Knobel, 1983). Our data are in general accordance with the previous studies, and also indicate a general trend in decreasing alkalinity, Eh, and pH along our studied flow path.

The concentrations of dissolved oxygen in groundwaters from Maryland's eastern shore and very low S(-II) concentrations indicate that these waters are generally suboxic with the exception of wells KE 66-0125 and QA 95-0611 that indicate oxic conditions (Berner, 1981). A key feature setting this aquifer apart from the Carrizo is that redox

41

conditions occurring within these groundwaters do not produce anoxic, or otherwise

sulfidic waters. Eh measurements are also consistent with the sub-oxic classifications

suggested by DO and S(-II) concentrations (Haque et al., 2008).

As indicated by previous studies, which are also in agreement with our findings,

the accumulation of NH_4^+ along the flow path is suggestive of post dissimilatory NO_3^-

reducing conditions prevailing in the Aquia groundwaters. The concentrations of total

iron (as well as its dissolved species) suggest that reduction of Fe(III) is an important

process in the aquifer (Haque et al., 2008). Elevated Fe_T and Fe(II) concentrations at

approximately 34 km along the flow path are an indication of Fe(III) reduction at this

location. Moreover, the high solubility of Fe(II), or rather the transition from Fe(III) to

Fe(II) is an indication of redox conditions being buffered by Fe (III) reduction as a result

of microbial dissimilatory Fe(III) reduction (Haque and Johannesson, 2007; Lovely et al.,

1990., Cummings et al., 1999).

6.2.2 Hydrogeochemical controls of W distribution in the Aquia groundwaters:

Evolution of W in the Aquia aquifer suggests the element's conservative behavior

in these generally oxic to suboxic groundwaters. Tungsten concentrations range from

14.31 to 184.41 pmol kg^{-1} indicating that these concentrations are much lower than those

obtained in the anoxic/sulfidic waters of the Carrizo Sand Aquifer, where concentrations

were as high as 1297 pmol kg^{-1}. Others have argued that W behaves conservatively in

well to moderately oxygenated waters (Johannesson et al., 2000, Annorsen and

Oskarssen., 2007). The observed changes of W concentrations along the studied flow

path is also consistent with some direct control due the moderately changing redox conditions in the aquifer, i.e from oxic, to suboxic conditions. For example, at approximately 33.5, 51.2, 64.5, and 86.3 km, relatively high W concentrations likely result from cycling of Fe in the aquifer, and increasing pH (Fig. 7, Table 5). The Aquia groundwaters generally have a pH greater than 6.5, and as a result, adsorbtion of W to Fe-hydroxides is likely to be especially for pH > 8. As noted above, for pH > 8, desorption of W into groundwaters should be important (Seiler et al., 2005), and previous studies indicate that W concentrations should increase at a pH greater than 8.2 because W desorbs from ferric hydroxides present in solution (Kenzendorf and Glassby., 1992; Seiler et al., 2005; Annorsen and Oskarssen., 2007). We suggest therefore that for W dissolution in groundwaters, pH related adsorption/ desorption reactions are the key controlling factors in oxic, and sub-oxic waters. We also suggest that areas of low W concentrations may reflect adsorption of W onto organic matter or clay minerals as well as ferric hydroxides thereby attributing to the low concentrations of W in the Aquia groundwaters.

6.2.3 Assessing mobilization of Tungsten from sequential extractions results:

The results of sequential extraction of Aquia sediments demonstrate that the oxidizable portion (tungsten bound to reduced metal complexes, or bound to organic matter) and the residual portion (tungsten held within the crystal structure of primary and secondary minerals) represent the major portion of total extractable tungsten. On the other hand, the exchangeable (labile), acidic (tungsten bound to sediment carbonates),

and reducible (tungsten bound to iron and manganese hydroxides) fractions represent the minor portion of total extractable tungsten. Previous studies on sequential extraction procedures indicate that W is roughly distributed equally in the residual and oxidizable fractions with minor amounts present in the other fractions (Koutsospyros et al.,2005) The high concentrations of tungsten in the last two fractions of our experiment (oxidizable and residual portions) are in accordance with these studies.

Our results also suggest that except for the first few sediment samples, most of the W in the Aquia sediments are bound up in Al-silicate minerals, and are therefore not available for recycling in the groundwaters. However, it seems that the most important source of W to these groundwaters is the 4th fraction (the oxidizable portion) which reflects W associated with organic matter or sulfide. It seems possible that oxidation of organic matter by dissimilatory respiring microbes may be in part responsible for some release of W to these groundwaters, or perhaps even the Fe(III) oxides in these sediments are sufficient to oxidize metal sulfide minerals containing W, and hence leading to the release of W into the water.

CHAPTER 7

CONCLUSIONS

According to the results obtained in this research project, naturally occurring W is present in groundwaters. The behavior of tungsten in groundwaters is dependent on a number of important factors that include: oxidation-reduction, adsorption-desorption, and precipitation-dissolution reactions/processes. In the Carrizo Sand aquifer, oxidizing conditions are found at the recharge zone of the aquifer around the first 15 km after which sulfidic/ anoxic conditions become prevalent. The Aquia aquifer fluctuated between oxic to suboxic conditions along the entire flowpath. Measurements of pH, alkalinity, dissolved iron species, S(-II) species, and oxidation-reduction potential along the respective flow paths are reflective of these conditions.

Tungsten concentrations in the Carrizo aquifer show a general and progressive increase as the waters become more sulfidic/anoxic. The measured tungsten values of the Carrizo Sand aquifer are notably much higher than those of the Aquia aquifer. In the Aquia groundwaters, tungsten behaves conservatively, and occurs in much lower concentrations such that they are reflective of the oxic to suboxic conditions of the aquifer. It is likely that the increase in tungsten concentrations in these aquifers are indicative of pH induced desorption/ dissolution of tungsten at higher pHs (> 8.2), and possible microbial dissimilatory processes. These results provide the initial insight of tungsten's behavior in two well-characterized aquifer groundwaters. Further research

incorporating the role of microbial activity will be beneficial in understanding the role of

tungsten in groundwaters in more detail.

REFERENCES

Appelo, C.A.J., 1994. A chromatographic model for water quality variations in the Aquia
    aquifer, Maryland, USA. Goldschmidt Conference Edinburgh. Faculty of Earth
    Sciences, De Boelelaan 1085, 1081 HV, Amsterdam, NL, pp. 23.

Arnorsson, S., Oskarsson, N., 2007. Molybdenum and tungsten in volcanic rocks and in
    surface and <100° C ground waters in Iceland. Geochim Cosmochim Acta 71,
    284-304.

Back, W., Barnes, I., 1965. Relation of electrochemical potentials and iron content to
    ground-water flow patterns. U.S Geol. Surv. Prof. Pap. 498-C, pp. 16.

Berner, R. A., 1981. A new geochemical classification of sedimentary environments. J.
    Sed. Petrol. 51, 359-365.

Castro, M.C., Goblet, P., 2003. Calibration of regional groundwater flow models:
    working hard toward a better understanding of site-specific systems. Water
    Resour. Res. 39(6), 1172, doi:10.1029/2002WR001653, 2003.

Castro, M.C., Stute, M., Schlosser, P., 2000. Comparison of 4 He ages and 14 C ages in
    simple aquifer systems: implications for groundwater flow and chronologies.
    Apppl. Geochem. 15, 1137-1167.

Champ, D.R., Oulens, J., Jackson, RE., 1979. Oxidation-reduction sequences in
    groundwater flow systems. Canadian J. Earth Sci. 16, 12-23.

Chapelle, F.H., 1983. Ground-water geochemistry and calcite cementation of the Aquia
auquifer in southern Maryland. Water Resour. Res. 19, 545-558.

Chapelle, F.H., Knobel, L.L., 1983. Aqueous geochemistry and the exchangeable cation
composition of glauconite in the Aquia aquifer, Maryland. Ground Water 21, 343-
352.

Cummings, D.E., Caccavo, Jr., F., Fendorf, S., Rosenzweif, R.F., 1999. Arsenic
Mobilization by the Dissililatory Fe(III)-reducing bacterium Shwangella alga
BrY. Environ. Sci. Technol. 33, 723-729.

Curtin, S.E., Andreaden, D.C., Wheeler, J.C., 2002. Potentiometric surface of the Aquia
in southern Maryland. USGS Open-file Report 2003 255.

Drummond, D.D., 2001. Hydrogeology of the Coastal Plain Aquifer System in Queen
Anne's and Talbot Counties, Maryland, with a Discussion of Brackish-Water
Intrusion in the Aquia Aquifer. Maryland Geological Survey, Report of
Investigations 72, USA.

Eaton, A.D., Clesceri, L.S., Greenberg, A.E. (ed.), 1995a. Standard methods for the
examination of water and wastewater. 3-67-68.

Edmunds, W.M.., Miles, D.L., Cook, J.M., 1984. A comparative study of sequential
redox processes in the three British aquifers. In: Eriksson E. (Ed.), Proceedings of
Hydrochemical Balances of Freshwater Systems, Uppsala Symposium. IAHS
Publication 150, pp. 55-70.

Hach, 2004. The Handbook DR/2400 Portable Spectrophotometer Procedure. USA.

Hamlin, S.H., 1988. Depositional and ground-water flow systems of the Carrizo-upper
Wilcox, South Texas. Report of Investigation-Texas, Bureau of Economic
Geology, Rept. Vol. 175, 61 pp.

Hansen, H.H., 1974. Sedimentary facies of the Aquia formation in the subsurface of the
Maryland Coastal Plain: Maryland Geological Survey Report of Investigations 21.

Haque, S., Johannesson, K.H., 2006a. Arsenic concentrations and speciation along a
groundwater flow path: the Carrizo Sand aquifer, Texas, USA. Chem. Geol. 228,
57-71.

Johannesson, K.H., Hendry, M.J., 2000. Rare earth element geochemistry of
groundwaters from a thick till clay-rich aquitard sequence, Saskatchewan,
Canada, Geochim. Cosmochim. Acta 64, 1493-1509.

Johannesson, K.H., Lyons, W.B., Graham, E.Y., Welch, K.A., 2000. Oxyanion
concentrations in Eastern Sierra Nevada rivers-3. Boron, Molybdenum,
Vanadium, and Tungsten. Aquatic Geochemistry 6, 19-46.

Kletzin, A., Adams, M.W.W., 1995. Tungsten in biological systems. FEMS
Microbiology Reviews, 5-63.

Koutsospyros, A., Braida, W., Christodoulastos, C., Dermatas, D., Strigul, N., 2006. A
review of tungsten: From environmental obscurity to scrutiny. Journal of
Hazardous Materials, 1-19.

Kunzendorf, H., Glasby, G.P., 1992. Tungsten accumulation in pacific ferro-manganese
deposits. Miner Deposita 27, 147-152.

Newsom, H.E., Sims, K.W.W., Noll Jr, P.D., Jaeger, W.L., Maehr, S.A., Beserra, T.B.,
1996. The depletion of tungsten in the bulk silicate earth: Constraints on core
formation. Geochim Cosmochim. Acta 60, 1155-1169.

Lovely, D.R., Chapelle, F.H., Phillips, E.J.P., 1990. Recovery of Fe(III)-reducing bacteria
from deeply buried sediments of the Atlanic coastal plain. Geology 18, 954-957.

Lovely, D.R., Goodwin, S., 1988. Hydrogen concentrations as an indicator of the
predominant terminal electron-accepting reactions in aquatic sediment. Geochim.
Cosmochim. Acta 52, 2993-3003.

Pearson, Jr., F.J., White D.E., 1967. Carbon 14 ages and flow rates of water in Carrizo
sand, Atascosa County, Texas. Water Resour. Res. 3, 251-261.

Seiler, R.L., Stollenwerk, K.G., Garbarino, J.R., 2005. Factors controlling tungsten
concentrations in ground water, Carson Desert, Nevada. Applied Geochemistry
20, 423-441.

Sheppard, P.R., Ridenour, G., Speakman, R.J., Witten, M.L., 2006. Elevated tungsten and
cobalt in airborne particulates in Fallon, Nevada: Possible implications for the
childhood leukemia cluster. Applied Geochemstry 21, 152-165.

Tang, J., Johannesson, K.H., 2006. Controls on the geochemistry of rare earth elements
along a groundwater flow path on the Carrizo Sand aquifer, Texas, USA.
Chemical Geology 225, 156-171.

Tang, J., Johannesson, K.H., 2005b. Adsorption of rare earth elements onto Carrizo sand:
Experimental investigations and modeling with surface complexation. Geochem.
Cosmochim. Acta. 69, 5247-2561.

Tang, J., Whittecar, G.r., Johannesson, K.H., Daniels, W.L., 2004. Potential contaminants
at a dredged spoil placement site, Charles City County, Virginia, as revealed by
sequential extraction. Transactions 5, 49-60.

Vessley, M.M., 2004. Chromiu along groundwater Flow Paths: The Carrizo Sand and
Upper Floridan aquifers, Texas and Florida, USA. Master's thesis, The University
of Texas at Arlington, Arlington, Texas.

BIOGRAPHICAL INFORMATION

Heeral Dave Champion, was born in Nairobi, Kenya, on August 16, 1982, the oldest daughter of Rita B. Dave and Bhadravadan I. Dave. She earned her Bachelor's Degree in Environmental Geology from The University of Texas at Arlington in 2005. Heeral had the opportunity to work as an intern with the United Nations Environmental Program (UNEP) in the Division of Policy Development and Law (DPDL) from June 2003 through August 2003. In 2006, she entered the Graduate School at The University of Texas at Arlington where she pursued her studies with the Department of Environmental Science and Engineering.

In May 2008, Heeral received the degree of Master's of Science in Environmental Science and Engineering. Heeral's research work, which addresses the hydrological and geochemical study of tungsten in groundwaters, is of great importance pertaining to its role as a possible concern to human health. Because little is known about the role of tungsten in groundwater systems, or the environment, her work will prove to be a significant contribution to the scientific community. Heeral plans on pursuing her interests in the Environmental Industry, specializing in groundwater geochemistry and natural resource management.